

# The Electroweak Phase Transition in Nearly Conformal Technicolor

James M. CLINE\*

*McGill University, Montréal, Québec H3A 2T8, Canada.*

Matti JÄRVINEN<sup>†</sup> and Francesco SANNINO<sup>‡</sup>

*High Energy Center, University of Southern Denmark,  
Campusvej 55, DK-5230 Odense M, Denmark.*

## Abstract

We examine the temperature-dependent electroweak phase transition in extensions of the Standard Model in which the electroweak symmetry is spontaneously broken via strongly coupled, nearly-conformal dynamics. In particular, we focus on the low energy effective theory used to describe Minimal Walking Technicolor at the phase transition. Using the one-loop effective potential with ring improvement, we identify significant regions of parameter space which yield a sufficiently strong first order transition for electroweak baryogenesis. The composite particle spectrum corresponding to these regions can be produced and studied at the Large Hadron Collider experiment. We note the possible emergence of a second phase transition at lower temperatures. This occurs when the underlying technicolor theory possesses a nontrivial center symmetry.

---

\*Electronic address: [jcline@hep.physics.mcgill.ca](mailto:jcline@hep.physics.mcgill.ca)

<sup>†</sup>Electronic address: [mjarvine@ifk.sdu.dk](mailto:mjarvine@ifk.sdu.dk)

<sup>‡</sup>Electronic address: [sannino@fysik.sdu.dk](mailto:sannino@fysik.sdu.dk)

## I. INTRODUCTION

The experimentally observed baryon asymmetry of the universe may be generated at the electroweak phase transition (EWPT) [1, 2, 3, 4, 5, 6, 7]. For the mechanism to be applicable it requires the presence of new physics beyond the Standard Model (SM) [8, 9, 10, 11, 12, 13]. An essential condition for electroweak baryogenesis is that the baryon-violating interactions induced by electroweak sphalerons are sufficiently slow immediately after the phase transition to avoid the destruction of the baryons that have just been created. This is achieved when the thermal average of the Higgs field evaluated on the ground state, in the broken phase of the electroweak symmetry, is large enough compared to the critical temperature at the time of the transition (see for example ref. [14] and references therein),

$$\phi_c/T_c > 1. \tag{1}$$

In the SM, the bound (1) was believed to be satisfied only for very light Higgs bosons [15, 16, 17, 18, 19]. However, this was before the mass of the top quark was known. With  $m_t = 175$  GeV, nonperturbative studies of the phase transition [20] show that the bound (1) cannot be satisfied for *any* value of the Higgs mass. In addition to the difficulties with producing a large enough initial baryon asymmetry, the impossibility of satisfying the sphaleron constraint (1) in the SM (Standard Model) provides an incentive for seeing whether the situation improves in various extensions of the SM. We refer to [14] for a summary of the different attempts in this direction.

In this paper we explore the electroweak phase transition in a model in which the electroweak symmetry is broken dynamically [21, 22]. A dynamical origin behind the spontaneous breaking of the electroweak symmetry is a natural extension of the SM. However, electroweak precision data and constraints from flavor changing neutral currents both disfavor an underlying gauge dynamics resembling too closely a scaled-up version of Quantum Chromodynamics (QCD) (see [23, 24, 25] for recent reviews).

Since technicolor models have been less fashionable than supersymmetric models in the last decade, it is worthwhile to review the recent progress that has enhanced their attractiveness from the particle physics perspective. One area of progress is in the understanding of the phase diagram [26, 27, 28, 29], as function of the number of flavors and colors, of

any  $SU(N)$  non-supersymmetric gauge theory with fermionic matter transforming according to various representations of the underlying gauge group. This has made it possible to provide the first classification of the possible theories one can use to break the electroweak symmetry [27, 36]. New analytic tools such as the all-order beta function [29] allow the determination, for the first time, of the anomalous dimension of the mass of the fermions at the nonperturbative infrared fixed point. This information is crucial for walking technicolor models [30, 31, 32, 33, 34, 35], *i.e.*, the ones for which the underlying gauge dynamics is nearly conformal.

A key realization that enabled further progress was that gauge theories with fermions in two-index (symmetric or adjoint) representations of the underlying gauge group have interesting features [26, 27, 28, 29, 36], such as the possibility of the existence of a nonperturbative infrared fixed point for a very low number of flavors [26], naturally reducing the tension with precision data [26, 36, 37, 38]. These properties make them intriguing candidates for walking technicolor type models [26, 36] (related studies can be found in [39]). In contrast, the naive scaling up of QCD, which is far from conformal, is strongly contradicted by phenomenological constraints [80].

Another important development occurred in first principle lattice simulations of the minimal walking technicolor theories, carried out in refs. [40, 41, 42, 43, 44]. These studies give preliminary support to the analytical arguments that these theories are near or actually already conformal. The case of fermions in the fundamental representation has been investigated in [40, 45, 46].

On the astrophysical side, technicolor models are capable of providing interesting dark matter candidates, since the new strong interactions confine techniquarks in technimeson and technibaryon bound states. The spin of the technibaryons depends on the representation according to which the technifermions transform, and the numbers of flavors and colors. The lightest technimeson is short-lived, thus evading BBN constraints, but the lightest technibaryon has typically [81] a mass of the order

$$m_{TB} \sim 1 - 2 \text{ TeV} . \tag{2}$$

Technibaryons are therefore natural dark matter candidates [47, 48, 49]. In fact it is possible to naturally understand the observed ratio of the dark to luminous matter mass

fraction of the universe if the technibaryon possesses an asymmetry [47, 48, 49]. If the latter is due to a net  $B - L$  generated at some high energy scale, then this would be subsequently distributed among *all* electroweak doublets by fermion-number violating processes in the SM at temperatures above the electroweak scale [50, 51, 52], thus naturally generating a technibaryon asymmetry as well. To avoid experimental constraints the technibaryon should be constructed in such a way as to be a complete singlet under the electroweak interactions [27, 48] while still having a nearly conformal underlying gauge theory [27]. In this case it would be hard to detect it in current earth-based experiments such as CDMS [49, 53, 54, 55, 56]. Other possibilities have been envisioned in [57, 58] and possible astrophysical effects studied in [59]. One can alternatively obtain dark matter from possible associated new sectors instead of the technicolor sector [60], including those which are not gauged under the electroweak interactions [27]. In [23] the reader will find an up-to-date summary of the recent efforts in this direction.

Coming to the main topic of this paper, the order of the electroweak phase transition (EWPT) depends on the underlying type of strong dynamics and plays an important role for baryogenesis [14, 61]. The technicolor chiral phase transition at finite temperature is mapped onto the electroweak one. Attention must be paid to the way in which the electroweak symmetry is embedded into the global symmetries of the underlying technicolor theory. An interesting preliminary analysis dedicated to earlier models of technicolor has been performed in [62].

In this work, we wish to investigate the EWPT in a class of realistic and viable technicolor models. An explicit phenomenological realization of walking models consistent with the electroweak precision data is termed Minimal Walking Technicolor (MWT) [37]. It is based on an  $SU(2)$  gauge theory coupled to two flavors of adjoint techniquarks. This model is thought to lie close, in theory space, to theories with nontrivial infrared fixed points [26, 29]. Indeed it is possible that it already has such a fixed point itself. In the vicinity of such a zero of the beta function, the coupling constant flows slowly (“walks”). This theory possesses an  $SU(4)$  global symmetry. At the LHC one will observe the composite states which are classified according to irreducible representations of the stability group left invariant by the technifermion condensate. The stability group, here, corresponds to the  $SO(4)$  symmetry which contains the  $SU(2)$  custodial symmetry of the SM. We choose the natural SM embedding, as detailed in the following section.

In ref. [37] a comprehensive Lagrangian was introduced for this model, taking into account the global symmetries of the underlying gauge theory, the walking dynamics via the modified Weinberg sum rules [63], and the constraints coming from precision data [38]. The effective theory contains composite scalars and spin-one vectors. Compatibility between the electroweak precision constraints and tree-level unitarity of  $WW$ -scattering was demonstrated in [64].

The study of longitudinal  $WW$  scattering unitarity versus precision measurements within the effective Lagrangian approach demonstrated that it is possible to pass the precision tests while simultaneously delaying the onset of unitarity [64].

In the present work we will use as a template the low energy effective theory developed in [37]. We start in section II by summarizing the basic theory, highlighting the degrees of freedom relevant near the phase transition. In section III the finite-temperature effective potential is then computed at the one-loop order, including the resummation of ring diagrams. Our analysis is presented in section IV. As a preliminary investigation we adopt the high-temperature expansion results for the effective potential. We then explore the region of the effective theory parameters yielding a first-order phase transition and study its strength. The ratio of the composite Higgs thermal expectation value at the critical temperature divided by the corresponding temperature is determined as function of the parameters of the low energy effective theory. We identify a significant region of parameter space where this ratio is sufficiently large to induce electroweak baryogenesis. The spectrum of the composite spin-zero states directly associated to these regions can be investigated and the related particles produced at the Large Hadron Collider experiment. In the subsection IV D we note the possible emergence of a second phase transition at lower temperatures, *i.e.*, the confinement/deconfinement one. This transition occurs when the underlying technicolor theory possesses a nontrivial center symmetry. Several appendices are provided, which give details concerning our analytical results.

## II. INTRODUCING MINIMAL WALKING TECHNICOLOR

### A. The underlying degrees of freedom and Lagrangian

The new dynamical sector we consider, which underlies the Higgs mechanism, is an  $SU(2)$  technicolor gauge theory with two adjoint technifermions [26]. The two adjoint fermions may be written as

$$Q_L^a = \begin{pmatrix} U^a \\ D^a \end{pmatrix}_L, \quad U_R^a, \quad D_R^a, \quad a = 1, 2, 3, \quad (3)$$

with  $a$  being the adjoint color index of  $SU(2)$ . The left-handed fields are arranged in three doublets of the  $SU(2)_L$  weak interactions in the standard fashion. The condensate is  $\langle \bar{U}U + \bar{D}D \rangle$  which correctly breaks the electroweak symmetry. The model as described so far suffers from the Witten topological anomaly [65]. However, this can easily be addressed by adding a new weakly charged fermionic doublet which is a technicolor singlet [36]. Schematically,

$$L_L = \begin{pmatrix} N \\ E \end{pmatrix}_L, \quad N_R, \quad E_R. \quad (4)$$

In general, the gauge anomalies cancel using the generic hypercharge assignment

$$Y(Q_L) = \frac{y}{2}, \quad Y(U_R, D_R) = \left( \frac{y+1}{2}, \frac{y-1}{2} \right), \quad (5)$$

$$Y(L_L) = -3\frac{y}{2}, \quad Y(N_R, E_R) = \left( \frac{-3y+1}{2}, \frac{-3y-1}{2} \right), \quad (6)$$

where the parameter  $y$  can take any real value [36]. In our notation the electric charge is  $Q = T_3 + Y$ , where  $T_3$  is the weak isospin generator. One recovers the SM hypercharge assignment for  $y = 1/3$ .

To discuss the symmetry properties of the theory it is convenient to use the Weyl basis for the fermions and arrange them in a vector transforming according to the fundamental

representation of SU(4),

$$Q = \begin{pmatrix} U_L \\ D_L \\ -i\sigma^2 U_R^* \\ -i\sigma^2 D_R^* \end{pmatrix}, \quad (7)$$

where  $U_L$  and  $D_L$  are the left-handed techniup and technidown, respectively, and  $U_R$  and  $D_R$  are the corresponding right-handed particles. Assuming the standard breaking to the maximal diagonal subgroup, the SU(4) symmetry spontaneously breaks to SO(4). This is driven by the condensate

$$\langle Q_i^\alpha Q_j^\beta \epsilon_{\alpha\beta} E^{ij} \rangle = -2 \langle \bar{U}_R U_L + \bar{D}_R D_L \rangle, \quad (8)$$

where the indices  $i, j = 1, \dots, 4$  denote the components of the tetraplet of  $Q$ , and the Greek indices indicate the ordinary spin. The matrix  $4 \times 4$   $E$  is defined in terms of the 2-dimensional unit matrix by

$$E = \begin{pmatrix} 0 & \mathbb{1} \\ \mathbb{1} & 0 \end{pmatrix}, \quad (9)$$

the antisymmetric tensor is  $\epsilon_{\alpha\beta} = -i\sigma_{\alpha\beta}^2$  and we used  $\langle U_L^\alpha U_R^{*\beta} \epsilon_{\alpha\beta} \rangle = -\langle \bar{U}_R U_L \rangle$ . A similar expression holds for the  $D$  techniquark. The above condensate is invariant under an SO(4) symmetry. This yields nine broken generators with associated Goldstone bosons.

Replacing the Higgs sector of the SM with MWT, one writes

$$\begin{aligned} \mathcal{L}_H \rightarrow & -\frac{1}{4} \mathcal{F}_{\mu\nu}^a \mathcal{F}^{a\mu\nu} + i\bar{Q}_L \gamma^\mu D_\mu Q_L + i\bar{U}_R \gamma^\mu D_\mu U_R + i\bar{D}_R \gamma^\mu D_\mu D_R \\ & + i\bar{L}_L \gamma^\mu D_\mu L_L + i\bar{N}_R \gamma^\mu D_\mu N_R + i\bar{E}_R \gamma^\mu D_\mu E_R \end{aligned} \quad (10)$$

with the technicolor field strength  $\mathcal{F}_{\mu\nu}^a = \partial_\mu \mathcal{A}_\nu^a - \partial_\nu \mathcal{A}_\mu^a + g_{TC} \epsilon^{abc} \mathcal{A}_\mu^b \mathcal{A}_\nu^c$ ,  $a, b, c = 1, \dots, 3$ . For the left-handed techniquarks the covariant derivative is

$$D_\mu Q_L^a = \left( \delta^{ac} \partial_\mu + g_{TC} \mathcal{A}_\mu^b \epsilon^{abc} - i\frac{g}{2} \vec{W}_\mu \cdot \vec{\tau} \delta^{ac} - ig' \frac{y}{2} B_\mu \delta^{ac} \right) Q_L^c. \quad (11)$$

Here  $\mathcal{A}_\mu$  are the techni gauge bosons,  $W_\mu$  are the gauge bosons associated to  $SU(2)_L$  and  $B_\mu$  is the gauge boson associated to the hypercharge.  $\tau^a$  are the Pauli matrices and  $\epsilon^{abc}$  is the fully antisymmetric symbol. In the case of right-handed techniquarks the third term containing the weak interactions disappears and the hypercharge  $y/2$  has to be replaced according to whether it is an up or down techniquark. For the left-handed leptons the second term containing the technicolor interactions disappears and  $y/2$  changes to  $-3y/2$ . Only the last term is present for the right-handed leptons with an appropriate hypercharge assignment.

## B. Tree Level Low Energy Theory for MWT

In [37] we constructed the effective theory for MWT including composite scalars and vector bosons, their self-interactions, and their interactions with the electroweak gauge fields and the SM fermions. We have also used the Weinberg modified sum rules to constrain the low energy effective theory. This extension of the SM was thereby shown to pass the electroweak precision tests. Near the finite temperature phase transition the relevant degrees of freedom are the scalars and hence we will not consider the vector spectrum nor that of the composite fermions.

### 1. Scalar Sector

The relevant effective theory for the Higgs sector at the electroweak scale consists, in our model, of a composite Higgs and its pseudoscalar partner, as well as nine pseudoscalar Goldstone bosons and their scalar partners. These can be assembled in the matrix

$$M = \left[ \frac{\sigma + i\Theta}{2} + \sqrt{2}(i\Pi^a + \tilde{\Pi}^a) X^a \right] E , \quad (12)$$

which transforms under the full  $SU(4)$  group according to

$$M \rightarrow uMu^T , \quad \text{with} \quad u \in SU(4) . \quad (13)$$



The  $X^a$ 's,  $a = 1, \dots, 9$  are the generators of the SU(4) group which do not leave the vacuum expectation value (VEV) of  $M$  invariant.  $\langle M \rangle$  is given by

$$\langle M \rangle = \frac{v}{2} E . \quad (14)$$

We note that  $\sigma$  is a scalar while the  $\Pi^a$ 's are pseudoscalars. It is convenient to separate the fifteen generators of SU(4) into the six that leave the vacuum invariant,  $S^a$ , and the remaining nine that do not,  $X^a$ .

The connection between the composite scalars and the underlying techniquarks can be derived from their transformation properties under SU(4), by observing that the elements of the matrix  $M$  transform like techniquark bilinears,

$$M_{ij} \sim Q_i^\alpha Q_j^\beta \varepsilon_{\alpha\beta} \quad \text{with } i, j = 1 \dots 4. \quad (15)$$

The electroweak subgroup can be embedded in SU(4), as explained in detail in [66]. The generators  $S^a$ , with  $a = 1, 2, 3$ , form a vectorial SU(2) subgroup of SU(4), which is denoted by SU(2)<sub>V</sub>, while  $S^4$  forms a U(1)<sub>V</sub> subgroup. The  $S^a$  generators, with  $a = 1, \dots, 4$ , together with the  $X^a$  generators, with  $a = 1, 2, 3$ , generate an SU(2)<sub>L</sub> × SU(2)<sub>R</sub> × U(1)<sub>V</sub> algebra. This is seen by changing generator basis from  $(S^a, X^a)$  to  $(L^a, R^a)$ , where

$$L^a \equiv \frac{S^a + X^a}{\sqrt{2}} = \begin{pmatrix} \frac{\tau^a}{2} & 0 \\ 0 & 0 \end{pmatrix}, \quad -R^{aT} \equiv \frac{S^a - X^a}{\sqrt{2}} = \begin{pmatrix} 0 & 0 \\ 0 & -\frac{\tau^{aT}}{2} \end{pmatrix}, \quad (16)$$

with  $a = 1, 2, 3$ . The electroweak gauge group is then obtained by gauging SU(2)<sub>L</sub> and the U(1)<sub>Y</sub> subgroup of SU(2)<sub>R</sub> × U(1)<sub>V</sub>, where

$$Y = -R^{3T} + \sqrt{2} Y_V S^4, \quad (17)$$

and  $Y_V$  is the U(1)<sub>V</sub> charge. For example, from eqs. (5) and (6) we see that  $Y_V = y$  for the techniquarks, and  $Y_V = -3y$  for the new leptons. As SU(4) spontaneously breaks to SO(4), SU(2)<sub>L</sub> × SU(2)<sub>R</sub> breaks to SU(2)<sub>V</sub>. As a consequence, the electroweak symmetry breaks to

$U(1)_Q$ , where

$$Q = \sqrt{2} S^3 + \sqrt{2} Y_V S^4 . \quad (18)$$

The  $SU(2)_V$  group, being entirely contained in the unbroken  $SO(4)$ , acts as a custodial isospin, which insures that the  $\rho$  parameter is equal to one at tree level.

The electroweak covariant derivative for the  $M$  matrix is

$$D_\mu M = \partial_\mu M - i g [G_\mu(y)M + MG_\mu^T(y)] , \quad (19)$$

where

$$\begin{aligned} g G_\mu(Y_V) &= g W_\mu^a L^a + g' B_\mu Y \\ &= g W_\mu^a L^a + g' B_\mu \left( -R^{3T} + \sqrt{2} Y_V S^4 \right) . \end{aligned} \quad (20)$$

Notice that in the last equation,  $G_\mu(Y_V)$  is written for a general  $U(1)_V$  charge  $Y_V$ , while in eq. (19) we have to take the  $U(1)_V$  charge of the techniquarks,  $Y_V = y$ , since these are the constituents of the matrix  $M$ , as explicitly shown in eq. (15).

Three of the nine Goldstone bosons associated with the broken generators become the longitudinal degrees of freedom of the massive weak gauge bosons, while the extra six Goldstone bosons will acquire a mass due to extended technicolor interactions (ETC) as well as the electroweak interactions *per se*. Using a bottom-up approach, we will not commit to a specific ETC theory, but rather limit ourselves to introducing the minimal low energy operators needed to construct a phenomenologically viable theory. The new Higgs Lagrangian is

$$\mathcal{L}_{\text{Higgs}} = \frac{1}{2} \text{Tr} [D_\mu M D^\mu M^\dagger] - \mathcal{V}(M) + \mathcal{L}_{\text{ETC}} , \quad (21)$$

where the potential reads

$$\begin{aligned} \mathcal{V}(M) &= -\frac{m^2}{2} \text{Tr}[MM^\dagger] + \frac{\lambda}{4} \text{Tr} [MM^\dagger]^2 + \lambda' \text{Tr} [MM^\dagger MM^\dagger] \\ &\quad - 2\lambda'' [\text{Det}(M) + \text{Det}(M^\dagger)] , \end{aligned} \quad (22)$$

and  $\mathcal{L}_{\text{ETC}}$  contains all terms which are generated by the ETC interactions, and not by the chiral symmetry breaking sector.

We explicitly break the SU(4) symmetry in order to provide mass to the Goldstone bosons which are not eaten by the weak gauge bosons. Assuming parity invariance,

$$\mathcal{L}_{\text{ETC}} = \frac{m_{\text{ETC}}^2}{4} \text{Tr} [MBM^\dagger B + MM^\dagger] + \dots , \quad (23)$$

where the ellipses represent possible higher dimensional operators, and  $B \equiv 2\sqrt{2}S^4$  commutes with the SU(2)<sub>L</sub> × SU(2)<sub>R</sub> × U(1)<sub>V</sub> generators.

The potential  $\mathcal{V}(M)$  is SU(4) invariant. It produces a VEV which parameterizes the techniquark condensate, and spontaneously breaks SU(4) to SO(4). In terms of the model parameters the VEV is

$$v^2 = \langle \sigma \rangle^2 = \frac{m^2}{\lambda + \lambda' - \lambda''} , \quad (24)$$

while the Higgs mass is

$$M_H^2 = 2 m^2 . \quad (25)$$

The linear combination  $\lambda + \lambda' - \lambda''$  corresponds to the Higgs self-coupling in the SM. The three pseudoscalar mesons  $\Pi^\pm, \Pi^0$ , correspond to the three massless Goldstone bosons which are absorbed by the longitudinal degrees of freedom of the  $W^\pm$  and  $Z$  boson. The remaining six uneaten Goldstone bosons are technibaryons, and all acquire tree-level degenerate masses through (not yet specified) ETC interactions:

$$M_{\Pi_{UU}}^2 = M_{\Pi_{UD}}^2 = M_{\Pi_{DD}}^2 = m_{\text{ETC}}^2 . \quad (26)$$

The remaining scalar and pseudoscalar masses are

$$\begin{aligned} M_\Theta^2 &= 4v^2\lambda'' \\ M_{A^\pm}^2 = M_{A^0}^2 &= 2v^2(\lambda' + \lambda'') \end{aligned} \quad (27)$$

for the technimesons, and

$$M_{\Pi UU}^2 = M_{\Pi UD}^2 = M_{\Pi DD}^2 = m_{\text{ETC}}^2 + 2v^2 (\lambda' + \lambda'') , \quad (28)$$

for the technibaryons. Ref. [67] provides further insight into some of these mass relations.

## 2. Fourth Lepton Family and Yukawa Interactions

The fermionic content of the effective theory consists of the SM quarks and leptons, the new lepton doublet  $L = (N, E)$  introduced to cure the Witten anomaly, and a composite techniquark-technigluon doublet. In fact the most relevant contributions are the ones of the top quark and the new lepton contribution due to their large Yukawa couplings and their relatively small zero-temperature masses, compared to the EWPT temperature.

Many extensions of technicolor have been suggested in the literature to provide masses to ordinary fermions. Some of the extensions use additional strongly coupled gauge dynamics, while others introduce fundamental scalars. Many variants of the schemes presented above exist, and a review of the major models is given by Hill and Simmons [24]. At the moment there is not yet a consensus on which ETC is the best. To keep the number of fields minimal, ref. [37] made the most economical ansatz, *i.e.*, ignorance of the complete ETC theory was parametrized by simply coupling the fermions to the low energy effective composite Higgs. This simple construction minimizes the flavor-changing neutral current problem. It is worth mentioning that it is possible to engineer a schematic ETC model proposed first by Randall in [68] and adapted for the MWT in [69] for which the effective theory presented here can be considered as a minimal description [82]. The details can be found in [37]. In our study of the phase transition we will not consider the composite fermions since they are expected to be much heavier than the scalar degrees of freedom.

## III. MWT - EFFECTIVE POTENTIAL

The tree-level effective potential is obtained by evaluating the potential in (22) and (23) in the background where the Higgs fields assumes the vacuum expectation value  $\sigma$ , *i.e.*,

$M = \sigma E/2$ . It has the SM form

$$V^{(0)} = \frac{1}{4} (\lambda + \lambda' - \lambda'') (\sigma^2 - v^2)^2 = \frac{M_H^2}{8v^2} (\sigma^2 - v^2)^2 . \quad (29)$$

The effective potential at one loop can be naturally divided into zero- and nonzero-temperature contributions.

### A. Zero Temperature Contribution

We begin by constructing the one-loop effective potential at zero temperature. We fix the counterterms so as to preserve the tree-level definitions of the VEV and the Higgs mass, *i.e.*,  $M_H^2 = 2\bar{\lambda}v^2$  with  $\bar{\lambda} = \lambda + \lambda' - \lambda''$ . The one loop contribution to the potential then reads:

$$V_{T=0}^{(1)} = \frac{1}{64\pi^2} \sum_i n_i f_i(M_i(\sigma)) + V_{\text{GB}} , \quad (30)$$

where the index  $i$  runs over all of the mass eigenstates, except for the Goldstone bosons (GB), and  $n_i$  is the multiplicity factor for a given scalar particle while for Dirac fermions is  $-4$  times the multiplicity factor of the specific fermion. The function  $f_i$  is:

$$f_i = M_i^4(\sigma) \left[ \log \frac{M_i^2(\sigma)}{M_i^2(v)} - \frac{3}{2} \right] + 2M_i^2(\sigma) M_i^2(v) , \quad (31)$$

where  $M_i^2(\sigma)$  is the background dependent mass term of the  $i$ -th particle. This prescription would lead to infrared divergences in the 't Hooft-Landau gauge for  $V_{\text{GB}}$ , the GB contribution, when evaluated at the tree-level VEV, due to the vanishing of the GB masses. Different ways of dealing with this problem have been discussed in the literature. One possibility is to regularize the infrared divergence by replacing  $M_i^2(v)$  with some characteristic mass scale. However with this prescription the tree-level VEV and Higgs mass get shifted by the presence of the one-loop correction. A simpler approach is to neglect the GB contribution, since in practice it never has a strong effect on the phase transition. We tried both methods and found that they give essentially indistinguishable results.

To explicitly evaluate the potential above it is useful to split the scalar matrix into four

$2 \times 2$  blocks as follows:

$$M = \begin{pmatrix} \mathcal{X} & \mathcal{O} \\ \mathcal{O}^T & \mathcal{Z} \end{pmatrix}, \quad (32)$$

with  $\mathcal{X}$  and  $\mathcal{Z}$  two complex symmetric matrices accounting for six independent degrees of freedom each and  $\mathcal{O}$  a generic complex  $2 \times 2$  matrix representing eight real bosonic fields.  $\mathcal{O}$  accounts for the SM-like Higgs doublet, a second doublet, and the three GB's absorbed by the longitudinal gauge bosons. We find  $n_{\mathcal{X}} = n_{\mathcal{Z}} = 6$  while the two weak doublets split into two  $SU(2)_V$  isoscalars, *i.e.*, the Higgs ( $n_H = 1$ ) and  $\Theta$  ( $n_{\Theta} = 1$ ) with different masses and two independent triplets, *i.e.*,  $n_{GB} = 3$  and  $n_A = 3$ . In Appendix A we summarize the tree-level expressions for the background-dependent masses of the scalar states.

For the contribution of the gauge bosons we have  $n_W = 6$  and  $n_Z = 3$ . In the fermionic sector we will consider only the heaviest particles, *i.e.*, the top for which  $n_T = -12$  and the two new leptons  $n_N = n_E = -4$ .

## B. One Loop Finite Temperature Effective Potential

The one-loop, ring-improved, finite-temperature effective potential can be divided into fermionic, scalar and vector contributions,

$$V_T^{(1)} = V_T^{(1)}{}_f + V_T^{(1)}{}_b + V_T^{(1)}{}_{\text{gauge}}. \quad (33)$$

The fermionic contribution at high temperature reads:

$$V_T^{(1)}{}_f = 2 \frac{T^2}{24} \sum_f n_f M_f^2(\sigma) + \frac{1}{16\pi^2} \sum_f n_f M_f^4(\sigma) \left[ \log \frac{M_f^2(\sigma)}{T^2} - c_f \right] \quad (34)$$

where  $c_f \simeq 2.63505$ ,  $n_{\text{Top}} = 3$ ,  $n_N = n_E = 1$ , and we have neglected  $\mathcal{O}(1/T^2)$  terms. The field-dependent masses are

$$M_{\text{Top}}(\sigma) = m_{\text{Top}} \frac{\sigma}{v}, \quad M_N(\sigma) = m_N \frac{\sigma}{v}, \quad M_E = m_E \frac{\sigma}{v}, \quad (35)$$

with  $m_{\text{Top}}$ ,  $m_N$  and  $m_E$  the physical masses. Notice that the logarithmic term in (34) combines with a similar term in the zero-temperature potential (30) so that their sum is

analytic in the masses  $M_f^2(\sigma)$ .

For the scalar part of the thermal potential one must resum the contribution of the ring diagrams. Following Arnold and Espinosa [17] we write

$$V_T^{(1)} = \frac{T^2}{24} \sum_b n_b M_b^2(\sigma) - \frac{T}{12\pi} \sum_b n_b M_b^3(\sigma, T) - \frac{1}{64\pi^2} \sum_b n_b M_b^4(\sigma) \left[ \log \frac{M_b^2(\sigma)}{T^2} - c_b \right], \quad (36)$$

where  $c_b \simeq 5.40762$  and  $M_b(\sigma, T)$  the thermal mass which follows from the tree-level plus one-loop thermal contribution to the potential (see Appendix A). For the gauge bosons,

$$V_T^{(1)}{}_{\text{gauge}} = \frac{T^2}{24} \sum_{gb} 3M_{gb}^2(\sigma) - \frac{T}{12\pi} \sum_{gb} [2M_{T,gb}^3(\sigma) + M_{L,gb}^3(\sigma, T)] - \frac{1}{64\pi^2} \sum_{gb} n_{gb} M_{gb}^4(\sigma) \left[ \log \frac{M_{gb}^2(\sigma)}{T^2} - c_b \right]. \quad (37)$$

Here  $M_{T,gb}$  ( $M_{L,gb}$ ) is the transverse (longitudinal) mass of a given gauge boson and we have  $M_{T,gb}(\sigma) = M_{L,gb}(\sigma, T = 0) = M_{gb}(\sigma)$ . Only the longitudinal gauge bosons acquire a thermal mass squared at the leading order,  $O(g^2 T^2)$ . The transverse bosons acquire instead a magnetic mass squared of order  $g^4 T^2$  which we have neglected.

The explicit form of the transverse and longitudinal gauge boson mass matrix is given in Appendix B.

#### IV. RESULTS

We used the one-loop high temperature approximation together with the summation of the ring-diagrams to evaluate the effective potential in our numerical calculations. The full expression of the finite temperature potential is given as a sum of the tree level potential (29), the zero-temperature one-loop contribution (30), and the one-loop thermal corrections at high temperature, (34), (36), and (37). We assumed that the phase transition takes place when the two minima are degenerate. This then defines the critical value of the thermal average of the composite Higgs field  $\phi_c$ , in the broken phase, at the critical temperature  $T_c$ . Above the critical temperature the ground state is the one at the origin of the Higgs field.

For convenience we subtracted from the potential a temperature-dependent constant which is defined in such a way that  $V(\sigma, T) = 0$  for  $\sigma = 0$ .

The relevant input parameters are the zero-temperature masses of the Higgs ( $M_H$ ) and its pseudoscalar partner  $\Theta$  ( $M_\Theta$ ). The phase transition also depends on the masses of the scalar partners of the Goldstone bosons  $A^{0,\pm}$  ( $M_A$ ), on the mass scale of the scalar baryons  $m_{\text{ETC}}$ , and on the masses of the heavy fermions. For simplicity, we choose the masses of the new fermions to be equal,

$$M_E^2 = M_N^2 \equiv M_f^2 . \quad (38)$$

This choice does not seem to have a strong effect on the phase transition; for example we checked that using instead  $M_E \simeq 2M_N$ , very similar results were obtained. We have neglected the heavy composite vectors of MWT since they are expected to decouple at the scale of the EWPT. At this scale, the couplings to the SM gauge bosons are simply  $g, g'$ . We set the parameter  $y$  to  $y = 1/3$  so that the MWT hypercharge assignment equals the SM one. Notice that  $y$  appears only in the longitudinal Debye mass of the  $Z$  boson. Since the effective potential terms are proportional to  $M_i^2(\sigma)$  or  $M_i^4(\sigma)$ , the contributions of the fermions and the composite scalars typically dominate over that of the relatively light  $Z$  boson, whence the dependence of the phase transition on  $y$  is negligible.

It is instructive to consider two limiting cases, for which the thermal mass spectrum simplifies: light and heavy ETC masses. Interpolating between these two cases would require some way of smoothly connecting the thermal masses when the heavy ETC states have decoupled, to those for which they are fully contributing. We discuss these separately in the following subsections.

### A. Heavy ETC-induced masses

We first consider  $\phi_c/T_c$  in the heavy ETC mass scenario, *i.e.*, taking the limit  $m_{\text{ETC}}/T_c \gg 1$ . When the scalar baryons become heavy their contributions to the effective potential become negligible. Since  $\phi_c/T_c$  is more sensitive to  $M_H$  and  $M_\Theta$  than to the other masses, we chose to plot it in the  $(M_H, M_\Theta)$  plane, while varying the remaining parameters  $M_A$  and  $M_f$ . The resulting dependences are shown in in fig. 1. The contour values of  $\phi_c/T_c$  are



$\phi_c/T_c = 0.5, \dots, 3.0$  from lighter to darker shades with steps of 0.5. Recall that electroweak baryogenesis requires  $\phi_c/T_c \gtrsim 1$ .

In the triangular regions in the upper left corners of the plots, the broken phase is metastable already at  $T = 0$ , whence there is no phase transition. When one approaches this region from below one observes that  $T_c$  goes to zero and  $\phi_c/T_c$  blows up. This happens since the one-loop zero-temperature potential induces an almost degenerate minimum at the origin together with the one at a finite value of  $\phi$ . At this point any small temperature favors the minimum at the origin. Such small temperatures are not within the range of applicability of the high-temperature expansion. It is for this reason that we excluded the region of parameter space yielding a one-loop zero-temperature potential with a global minimum at the origin.

We observe a similar behavior in the region of parameter space where  $M_H \simeq 120$  GeV and  $M_\Theta \simeq 650$  GeV in the  $M_A = 350$  GeV,  $M_f = 350$  GeV plot. In this case the black and white regions cannot be studied via the high-temperature approximation since  $M_\Theta/T_c > 7$ , which is a strong indication of the breakdown of the high-temperature expansion [83]. However, we have checked the validity of the high- $T$  expansion for the other regions of our plots by adding higher order terms in the expansion and seeing how the results change. Including terms up to and including order  $1/T^6$ , we find that the quantitative results presented here are stable against higher order corrections.

## B. Light ETC-induced masses

In the light ETC mass scenario, all of the MWT scalars are relatively light with respect to the electroweak scale. Then all the degrees of freedom which were discussed in Subsection III A are thermally active at the phase transition. The strength of the phase transition in this case is plotted in fig. 2. Since we found  $\phi_c/T_c$  to be rather weakly dependent on  $m_{\text{ETC}}$  when the scalar baryons are thermally active, we fixed  $m_{\text{ETC}} = 150$  GeV. The transition is slightly weaker than in the heavy  $m_{\text{ETC}}$  scenario. For  $M_A \gtrsim 300$  GeV or  $M_f \gtrsim 500$  GeV no first order transition is seen. This is why we changed the second reference point of  $M_A$  from 350 GeV to 250 GeV in the plots.

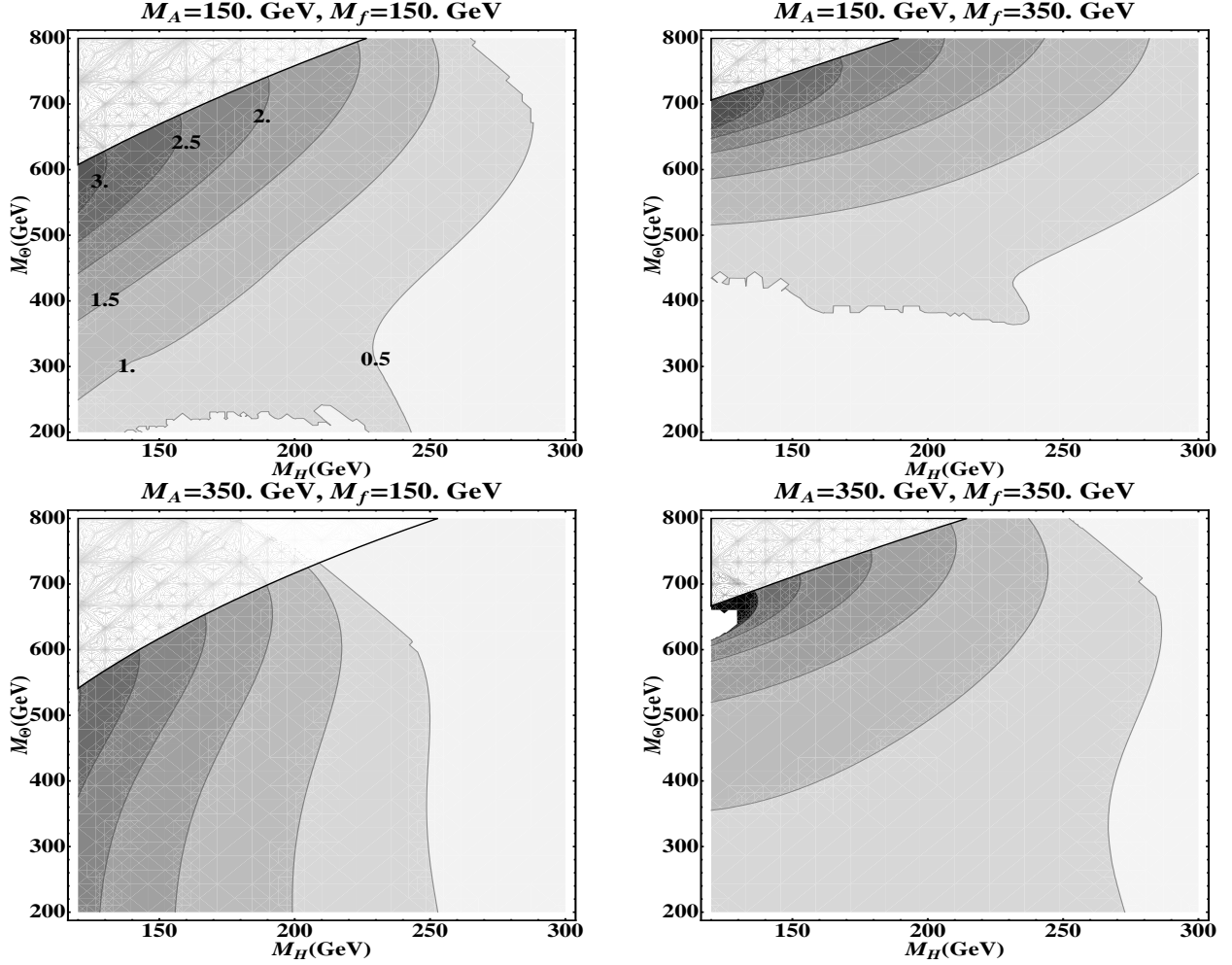


FIG. 1: The strength of the phase transition ( $\phi_c/T_c$ ) in the  $M_H$ - $M_\Theta$  plane for  $M_A$ ,  $M_f = 150$  GeV and 300 GeV, in the heavy ETC mass scenario.  $\phi_c/T_c = 0.5, 1.0, 1.5, \dots 3.0$  at the contour lines, such that  $\phi_c/T_c < 0.5$  in the region with lightest color. In the white region in the upper left corners of the plots the broken phase vacuum is metastable already at  $T = 0$ .

### C. Explanation of Results

It is possible to qualitatively understand the behavior of  $\phi_c/T_c$  as a function of the masses. In general, a strong first order phase transition can be achieved if the zero-temperature potential is close to being flat, *i.e.*, the vacuum value  $V(\sigma = v)$  is small and negative (recall that we define  $V(\sigma = 0)$  to be zero). Then if the thermal corrections are strong and positive around  $\sigma \simeq v$ , the phase transition takes place at a low temperature, giving a large  $\phi_c/T_c$ .

In our model  $V(\sigma = v)$  is small typically when the composite Higgs mass is low and one of the masses  $M_A$  and  $M_\Theta$  is a bit larger. The one-loop zero-temperature contribution

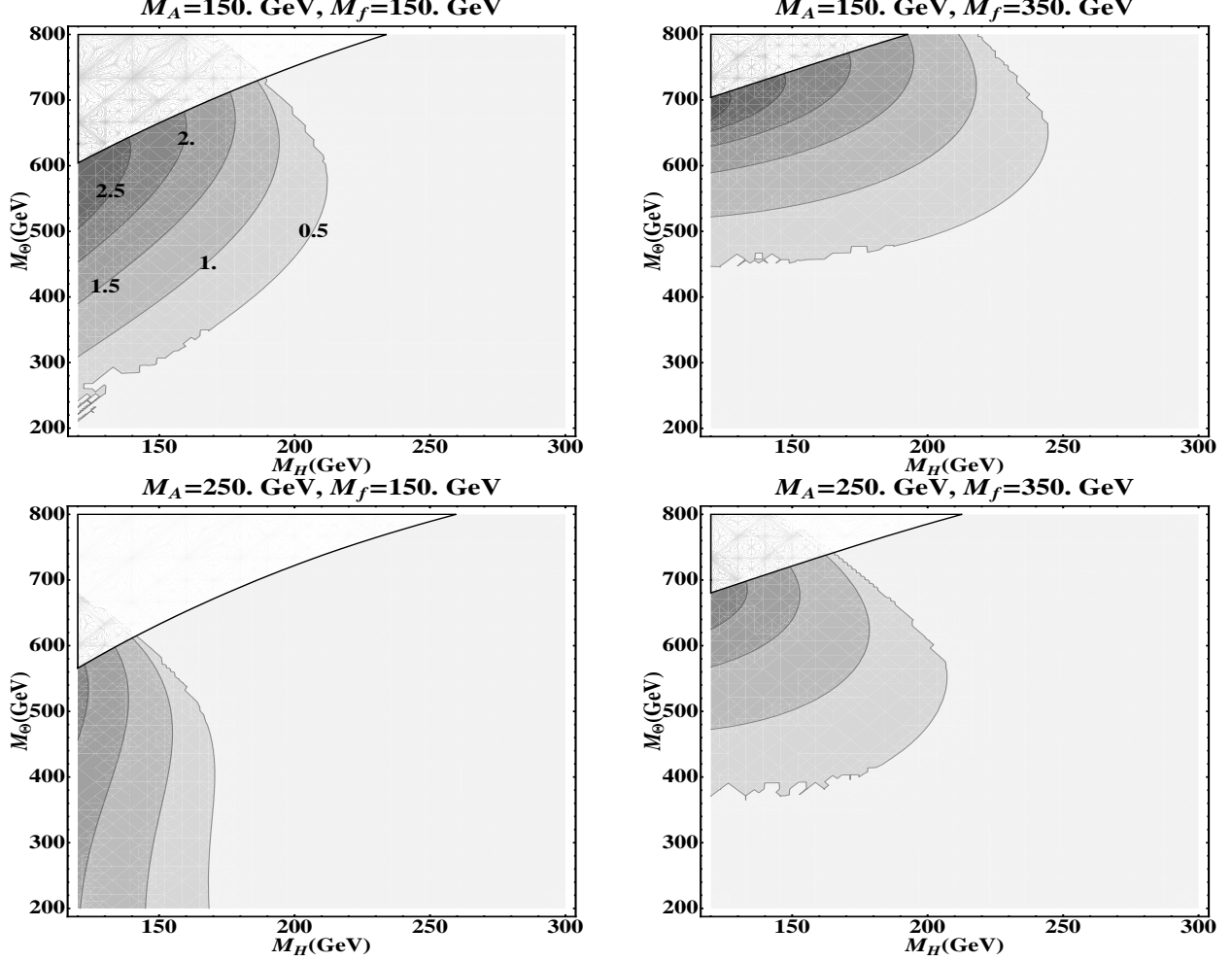


FIG. 2: The strength of the phase transition ( $\phi_c/T_c$ ) in the  $M_H$ - $M_\Theta$  plane, for the light ETC mass ( $m_{\text{ETC}} = 150$  GeV) scenario.  $M_A$  and  $M_f$  are varied as indicated in the labels.

of the scalars is enhanced relative to the tree-level potential for such values of the masses. It increases the value of the potential at the broken phase and creates a bump between the two minima. This is illustrated in figure 3, which shows the typical shape of the one-loop correction (30,31) from bosons, where we have replaced  $\log(m^2(\sigma))$  by  $\log(T^2)$  due to the finite- $T$  contribution canceling this nonanalytic dependence. Fermions have exactly the opposite effect, whence the contributions of the fermions and the scalar bosons need to be balanced. The baryons do not play a big role, since their (squared) masses include the hard term  $M_{\text{ETC}}^2$  and are thus more weakly dependent on  $\sigma$ .

The shape of the thermal corrections also affects  $\phi_c/T_c$ , since a term of the form  $-Tm^3 \sim -T\phi^3$  creates a barrier between the symmetric and broken phases in the potential at the

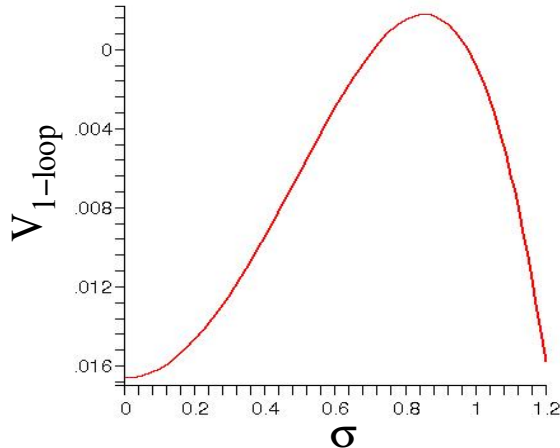


FIG. 3: Typical shape of bosonic contribution to one-loop zero temperature potential, eqs. (30,31), which helps to enhance the strength of the phase transition.

critical temperature, where  $V \sim \lambda\phi^2(\phi - v_c)^2$ . However this is only true if the field-dependent mass is close to the form  $m^2 \sim g^2\phi^2$ . Thermal and vacuum contributions of the form  $m^2 \sim g^2\phi^2 + m_0^2(T)$  reduce this effect, and for large  $m_0^2(T)$ , the expansion of the cubic term in powers of  $\phi$  gives contributions in the wrong direction, tending to reduce  $\phi_c/T_c$ .

The behavior seen in figs. 1 and 2 can be understood as a combination of the above effects. In the white regions in the upper left-hand corners of the plots, the contribution to the bump from the zero- $T$  one-loop correction is so large that the broken-phase vacuum is metastable even at  $T = 0$ . Next to this region there is a large part of parameter space where the scalar and fermion masses are correctly balanced to produce small and negative  $V(\sigma = v)$ , which yields large  $\phi_c/T_c$ . However, in the upper right-hand corner of the plots,  $\sum_b n_b M_b^2$  becomes so large that the thermal corrections do not enhance the potential at  $\sigma \simeq v$  any longer, and the phase transition is weakened. When the composite baryons are thermally active (light ETC masses), their effect on the ring resummation makes the second term of (36) more negative, but not sufficiently of the form  $\phi^3$ . Hence the scalar and Higgs masses are restricted to be smaller to compensate, which causes the difference between figs. 1 and 2.

Note that when the scalar baryons are decoupled, the scalar fields of MWT consist of two Higgs doublets. Hence dependences shown in figs. 1 and 2 are quite similar to those of the two Higgs doublet models [76]. Both have a metastable broken phase vacuum when the Higgs is light and the other scalars are heavy with respect to the electroweak scale. The

edge of this region has a similar dependence on  $M_H$  in both models. Strong first order phase transitions are observed near the regions of metastable vacua in both cases.

In the parameter region where a strong first order transition is observed the composite Higgs and its pseudoscalar partner  $\Theta$  are light enough to be produced at the LHC. Moreover one expects, for this range of parameters of the effective Lagrangian, sizable deviations from the SM predictions at the LHC. For example, the important  $pp \rightarrow HW$  process at LHC is enhanced relative to the SM one [77]. A detailed analysis dedicated to the LHC phenomenology of nearly-conformal technicolor models is about to appear [78]. We emphasize that the spectrum is completely fixed by the underlying gauge theory and that first principle lattice simulations can test our results.

#### **D. A novel phase transition at lower energies**

As suggested in [23], an intriguing possibility can emerge in that one can have *two independent* phase transitions at nonzero temperature in technicolor theories, whenever the theory possesses a nontrivial center symmetry. The two phase transitions are the chiral one, directly related to the electroweak phase transition, and a confining one at lower temperatures. During the history of the universe one predicts a phase transition around the electroweak scale and another one at lower temperatures with a jump in the entropy proportional to the number of degrees of freedom liberated (or gapped) when increasing (decreasing) the temperature (see [79] for a simple explanation of this phenomenon and a list of relevant references). This may have very interesting cosmological consequences. In this work we have concentrated on the chiral one alone. The interplay with the confining one, expected to occur at lower temperatures, can be studied by coupling the effective Lagrangian presented here to the Polyakov-loop effective degree of freedom as done in [79].

#### **Acknowledgments**

J.C. is supported by NSERC of Canada. The work of M.J. and F.S. is supported by the Marie Curie Excellence Grant under contract MEXT-CT-2004-013510. We thank the CERN theory group for its hospitality during the initiation of this work.

## APPENDIX A: ZERO- AND FINITE-TEMPERATURE BACKGROUND DEPENDENT SCALAR MASSES

The composite scalars are assembled in the matrix  $M$  of Eq. (12). In terms of the mass eigenstates this reads

$$M = \begin{pmatrix} i\Pi_{UU} + \tilde{\Pi}_{UU} & \frac{i\Pi_{UD} + \tilde{\Pi}_{UD}}{\sqrt{2}} & \frac{\sigma + i\Theta + i\Pi^0 + A^0}{2} & \frac{i\Pi^+ + A^+}{\sqrt{2}} \\ \frac{i\Pi_{UD} + \tilde{\Pi}_{UD}}{\sqrt{2}} & i\Pi_{DD} + \tilde{\Pi}_{DD} & \frac{i\Pi^- + A^-}{\sqrt{2}} & \frac{\sigma + i\Theta - i\Pi^0 - A^0}{2} \\ \frac{\sigma + i\Theta + i\Pi^0 + A^0}{2} & \frac{i\Pi^- + A^-}{\sqrt{2}} & i\Pi_{\overline{UU}} + \tilde{\Pi}_{\overline{UU}} & \frac{i\Pi_{\overline{UD}} + \tilde{\Pi}_{\overline{UD}}}{\sqrt{2}} \\ \frac{i\Pi^+ + A^+}{\sqrt{2}} & \frac{\sigma + i\Theta - i\Pi^0 - A^0}{2} & \frac{i\Pi_{\overline{UD}} + \tilde{\Pi}_{\overline{UD}}}{\sqrt{2}} & i\Pi_{\overline{DD}} + \tilde{\Pi}_{\overline{DD}} \end{pmatrix}, \quad (\text{A1})$$

where  $\sigma = v + H$ . The Lagrangian summary for the Higgs sector, including the spontaneously broken potential, and the ETC mass term for the uneaten Goldstone bosons, is

$$\begin{aligned} \mathcal{L}_{\text{Higgs}} &= \frac{1}{2} \text{Tr} [D_\mu M D^\mu M^\dagger] + \frac{m^2}{2} \text{Tr} [M M^\dagger] \\ &\quad - \frac{\lambda}{4} \text{Tr} [M M^\dagger]^2 - \lambda' \text{Tr} [M M^\dagger M M^\dagger] + 2\lambda'' [\text{Det}(M) + \text{Det}(M^\dagger)] \\ &\quad + \frac{m_{\text{ETC}}^2}{4} \text{Tr} [M B M^\dagger B + M M^\dagger], \end{aligned} \quad (\text{A2})$$

where the covariant derivative is given by Eq. (19).

The zero-temperature background-dependent scalar mass squared eigenstates are:

$$\begin{aligned}
& -m^2 + m_{ETC}^2 + (\lambda - \lambda'' + \lambda') \sigma^2 \quad , \quad 6 \text{ degenerate states} \\
& -m^2 + m_{ETC}^2 + (\lambda + \lambda'' + 3\lambda') \sigma^2 \quad , \quad 6 \text{ degenerate states} \\
& \quad -m^2 + (\lambda - \lambda'' + \lambda') \sigma^2 \quad , \quad 3 \text{ degenerate states (GB)} \\
& \quad -m^2 + (\lambda + \lambda'' + 3\lambda') \sigma^2 \quad , \quad 3 \text{ degenerate states} \\
& \quad -m^2 + 3(\lambda - \lambda'' + \lambda') \sigma^2 \quad , \quad 1 \text{ state (Higgs)} \\
& \quad -m^2 + (\lambda + 3\lambda'' + \lambda') \sigma^2 \quad , \quad 1 \text{ state}
\end{aligned} \tag{A3}$$

The temperature-dependent (one-loop) effective scalar masses of the Arnold-Espinosa approximation [17] are calculated as follows. Compute the  $T^2$  term of the one-loop thermal correction  $V_T^{(1)}$  as explained in subsection III B, but in an arbitrary background, *i.e.*, function of all the scalar fields. Then, for example, the contribution of the top quark loop reads

$$V_{T^2 \text{ Top}}^{(1)} = \frac{T^2}{4} M_{\text{Top}}^2 \Big|_{\text{background}} = \frac{m_{\text{Top}}^2 T^2 ((\Theta + \Pi^0)^2 + (\sigma + A^0)^2)}{4v^2} . \tag{A4}$$

The effective thermal masses are obtained by adding to the  $T = 0$  scalar mass matrix the thermal mass matrix

$$M_{ij} = \frac{\partial^2}{\partial v_i \partial v_j} V_{T^2}^{(1)} . \tag{A5}$$

Here  $v_i$  represents the  $i$ -th scalar field thermally active at the electroweak phase transition.

The one-loop finite-temperature correction to the scalar masses, due solely to the scalar self-interactions, and considering all of the 20 bosons to be thermally active, is

$$\frac{T^2}{6} (11\lambda + 20\lambda') . \tag{A6}$$

However the full finite-temperature corrections have involved expressions when taking into account all the particles, *i.e.*, gauge bosons and fermions.

We summarize below the temperature and background dependent scalar masses in the case in which the ETC states are heavy, and hence integrated out, and the case in which we retain all of the states.

1. **Heavy**  $M_{etc}$

$$M_{\Pi^\pm}^2(\sigma, T) = -m^2 + (\lambda + \lambda' - \lambda'')\sigma^2 + \frac{T^2}{6}(5\lambda + 8\lambda') + \frac{T^2}{16}(g_1^2 + 3g_2^2) \quad (\text{A7})$$

$$M_{A^\pm}^2(\sigma, T) = -m^2 + (\lambda + 3\lambda' + \lambda'')\sigma^2 + \frac{T^2}{6}(5\lambda + 8\lambda') + \frac{T^2}{16}(g_1^2 + 3g_2^2) \quad (\text{A8})$$

$$\begin{aligned} M_{\Theta/\Pi^0}^2(\sigma, T) &= -m^2 + (\lambda + \lambda' + \lambda'')\sigma^2 \\ &+ \frac{T^2}{6}(5\lambda + 8\lambda') + \frac{T^2}{16}(g_1^2 + 3g_2^2) + \frac{T^2}{6v^2}(m_E^2 + m_N^2 + 3m_{\text{Top}}^2) \\ &\pm \sqrt{(2\lambda''\sigma^2)^2 + \left[ \frac{T^2}{6v^2}(-m_E^2 + m_N^2 + 3m_{\text{Top}}^2) \right]^2} \end{aligned} \quad (\text{A9})$$

$$\begin{aligned} M_{H/A^0}^2(\sigma, T) &= -m^2 + (2\lambda + 3\lambda' - \lambda'')\sigma^2 \\ &+ \frac{T^2}{6}(5\lambda + 8\lambda') + \frac{T^2}{16}(g_1^2 + 3g_2^2) + \frac{T^2}{6v^2}(m_E^2 + m_N^2 + 3m_{\text{Top}}^2) \\ &\pm \sqrt{[(\lambda - 2\lambda'')\sigma^2]^2 + \left[ \frac{T^2}{6v^2}(-m_E^2 + m_N^2 + 3m_{\text{Top}}^2) \right]^2} \end{aligned} \quad (\text{A10})$$

2. **Light**  $M_{etc}$

$$M_{\Pi^\pm}^2(\sigma, T) = -m^2 + (\lambda + \lambda' - \lambda'')\sigma^2 + \frac{T^2}{6}(11\lambda + 20\lambda') + \frac{T^2}{16}(g_1^2 + 3g_2^2) \quad (\text{A11})$$

$$M_{A^\pm}^2(\sigma, T) = -m^2 + (\lambda + 3\lambda' + \lambda'')\sigma^2 + \frac{T^2}{6}(11\lambda + 20\lambda') + \frac{T^2}{16}(g_1^2 + 3g_2^2) \quad (\text{A12})$$



$$\begin{aligned}
M_{\Theta/\Pi^0}^2(\sigma, T) &= -m^2 + (\lambda + \lambda' + \lambda'')\sigma^2 \\
&+ \frac{T^2}{6}(11\lambda + 20\lambda') + \frac{T^2}{16}(g_1^2 + 3g_2^2) + \frac{T^2}{6v^2}(m_E^2 + m_N^2 + 3m_{\text{Top}}^2) \\
&\pm \sqrt{(2\lambda''\sigma^2)^2 + \left[ \frac{T^2}{6v^2}(-m_E^2 + m_N^2 + 3m_{\text{Top}}^2) \right]^2}
\end{aligned} \tag{A13}$$

$$\begin{aligned}
M_{H/A^0}^2(\sigma, T) &= -m^2 + (2\lambda + 3\lambda' - \lambda'')\sigma^2 \\
&+ \frac{T^2}{6}(11\lambda + 20\lambda') + \frac{T^2}{16}(g_1^2 + 3g_2^2) + \frac{T^2}{6v^2}(m_E^2 + m_N^2 + 3m_{\text{Top}}^2) \\
&\pm \sqrt{[(\lambda - 2\lambda'')\sigma^2]^2 + \left[ \frac{T^2}{6v^2}(-m_E^2 + m_N^2 + 3m_{\text{Top}}^2) \right]^2}
\end{aligned} \tag{A14}$$

$$\begin{aligned}
M_{\Pi_{UD}/\tilde{\Pi}_{UD}}^2(\sigma, T) &= -m^2 + m_{\text{ETC}}^2 + (\lambda + 2\lambda')\sigma^2 + \frac{T^2}{6}(11\lambda + 20\lambda') + \frac{T^2}{4}(y^2 g_1^2 + g_2^2) \\
&\pm \sqrt{[(\lambda' + \lambda'')\sigma^2]^2 + \left( \frac{1}{4}T^2 g_2^2 \right)^2}
\end{aligned} \tag{A15}$$

$$\begin{aligned}
M_{\Pi_{UU}/\tilde{\Pi}_{UU}}^2(\sigma, T) &= -m^2 + m_{\text{ETC}}^2 + (\lambda + 2\lambda')\sigma^2 + \frac{T^2}{6}(11\lambda + 20\lambda') \\
&+ \frac{T^2}{8}[(1 + 2y + 2y^2)g_1^2 + 2g_2^2] \\
&\pm \sqrt{[(\lambda' + \lambda'')\sigma^2]^2 + \left\{ \frac{T^2}{8}[(1 + 2y)g_1^2 - 2g_2^2] \right\}^2}
\end{aligned} \tag{A16}$$

$$\begin{aligned}
M_{\Pi_{DD}/\tilde{\Pi}_{DD}}^2(\sigma, T) &= -m^2 + m_{\text{ETC}}^2 + (\lambda + 2\lambda')\sigma^2 + \frac{T^2}{6}(11\lambda + 20\lambda') \\
&+ \frac{T^2}{8}[(1 - 2y + 2y^2)g_1^2 + 2g_2^2] \\
&\pm \sqrt{[(\lambda' + \lambda'')\sigma^2]^2 + \left\{ \frac{T^2}{8}[(1 - 2y)g_1^2 - 2g_2^2] \right\}^2}
\end{aligned} \tag{A17}$$

Here the notation  $M_{A/B}$  means that the states  $A$  and  $B$  are mixed through thermal corrections. The diagonal thermal masses of each  $A/B$  system are reported on the right hand side.

**APPENDIX B: TRANSVERSE AND LONGITUDINAL GAUGE BOSON MASS MATRIX**

The background dependent transverse gauge boson mass matrix is:

$$M_T^2(\sigma) = \frac{\sigma^2}{4} \begin{bmatrix} g^2 & 0 & 0 & 0 \\ 0 & g^2 & 0 & 0 \\ 0 & 0 & g^2 & -g'g \\ 0 & 0 & -g'g & g'^2 \end{bmatrix}, \quad (\text{B1})$$

while the longitudinal background dependent Debye mass is in MWT:

$$M_L^2(\sigma) = M_T^2(\sigma) + \Pi_L, \quad (\text{B2})$$

with

$$\Pi_L = \begin{bmatrix} (2 + \frac{5}{6})g^2T^2 & 0 & 0 & 0 \\ 0 & (2 + \frac{5}{6})g^2T^2 & 0 & 0 \\ 0 & 0 & (2 + \frac{5}{6})g^2T^2 & 0 \\ 0 & 0 & 0 & f(y)g'^2T^2 \end{bmatrix}, \quad (\text{B3})$$

and  $3f(y) = 1 + (6y^2 + 2) + 5 + \frac{1}{2}(9y^2 + \frac{1}{2}) + \frac{1}{2}(y^2 + \frac{1}{2})$ . The longitudinal mass matrix receives finite temperature contributions from the scalars, the new lepton family, the techniquark-technigluon states which adds to the usual SM corrections (but with the standard Higgs replaced by the technicolor sector). The transverse bosons acquire a magnetic mass of order  $g^2T$  which we have neglected. To compute the nonzero temperature corrections to the longitudinal vector boson masses we have used the formulae:

$$\underline{U(1)} \quad \Pi_L^S = \frac{g'^2T^2}{3} \sum_S Y_S^2, \quad \Pi_L^F = \frac{g'^2T^2}{6} \sum_F Y_F^2 \quad (\text{B4})$$

where the sums are over complex scalars and chiral fermions respectively. For the nonabelian part we used:

$$\underline{SU(N)} \quad \Pi_L^S = \frac{g^2T^2}{3} \sum_S t_2(R_S), \quad \Pi_L^F = \frac{g^2T^2}{6} \sum_F t_2(R_F), \quad \Pi_L^V = \frac{N}{3}g^2T^2, \quad (\text{B5})$$

where  $\delta^{ab}t_2(R) = \text{Tr} [T^a T^b]$ . It is instructive to separate the various contributions to  $\Pi_L$ .

For the  $U(1)$  part the fermionic and scalar contributions read:

$$\Pi_L^F = T^2 g'^2 \left[ \frac{5}{9} N_g + \frac{18y^2 + 1}{12} + \frac{2y^2 + 1}{12} \right], \quad (\text{B6})$$

$$\Pi_L^S = \frac{T^2 g'^2}{3} [1 + (6y^2 + 2)] \quad (\text{B7})$$

where the first contribution counts  $N_g = 3$  generations of the SM fermions, the second contribution is due to the new non technicolor family while the last term is due to the techniquark-technigluon fermion states. For the bosonic sector the first term is due to the two Higgs doublets contained in  $\mathcal{O}$  while the term in brackets takes into account the contribution of the other di-techniquark type of states.

For the  $SU(2)$  part the fermionic, scalar and vector contributions reads:

$$\Pi_L^F = \frac{T^2 g^2}{6} \left[ 2N_g + \frac{1}{2} + \frac{1}{2} \right], \quad (\text{B8})$$

$$\Pi_L^S = \frac{T^2 g^2}{3} [1 + 2], \quad (\text{B9})$$

$$\Pi_L^V = \frac{2}{3} T^2 g^2. \quad (\text{B10})$$

In the fermionic case the first contribution counts  $N_g = 3$  generations of the SM fermions, the second contribution is due to the new non technicolor family while the last term is due to the techniquark-technigluon fermion states. For the bosonic sector the first term is due to the two Higgs doublets contained in  $\mathcal{O}$  while the term in brackets takes into account the contribution of the other di-techniquark type of states (the ones in the upper left component of the matrix  $M$ ).

### APPENDIX C: GENERATORS

It is convenient to use the following representation of  $SU(4)$

$$S^a = \begin{pmatrix} \mathbf{A} & \mathbf{B} \\ \mathbf{B}^\dagger & -\mathbf{A}^T \end{pmatrix}, \quad X^i = \begin{pmatrix} \mathbf{C} & \mathbf{D} \\ \mathbf{D}^\dagger & \mathbf{C}^T \end{pmatrix}, \quad (\text{C1})$$

where  $A$  is hermitian,  $C$  is hermitian and traceless,  $B = -B^T$  and  $D = D^T$ . The  $S$  are also a representation of the  $SO(4)$  generators, and thus leave the vacuum invariant  $S^a E + E S^{aT} = 0$ . Explicitly, the generators read

$$S^a = \frac{1}{2\sqrt{2}} \begin{pmatrix} \tau^a & \mathbf{0} \\ \mathbf{0} & -\tau^{aT} \end{pmatrix}, \quad a = 1, \dots, 4, \quad (\text{C2})$$

where  $a = 1, 2, 3$  are the Pauli matrices and  $\tau^4 = \mathbb{1}$ . These are the generators of  $SU_V(2) \times U_V(1)$ .

$$S^a = \frac{1}{2\sqrt{2}} \begin{pmatrix} \mathbf{0} & \mathbf{B}^a \\ \mathbf{B}^{a\dagger} & \mathbf{0} \end{pmatrix}, \quad a = 5, 6, \quad (\text{C3})$$

with

$$B^5 = \tau^2, \quad B^6 = i\tau^2. \quad (\text{C4})$$

The rest of the generators which do not leave the vacuum invariant are

$$X^i = \frac{1}{2\sqrt{2}} \begin{pmatrix} \tau^i & \mathbf{0} \\ \mathbf{0} & \tau^{iT} \end{pmatrix}, \quad i = 1, 2, 3, \quad (\text{C5})$$

and

$$X^i = \frac{1}{2\sqrt{2}} \begin{pmatrix} \mathbf{0} & \mathbf{D}^i \\ \mathbf{D}^{i\dagger} & \mathbf{0} \end{pmatrix}, \quad i = 4, \dots, 9, \quad (\text{C6})$$

with

$$\begin{aligned} D^4 &= \mathbb{1}, & D^6 &= \tau^3, & D^8 &= \tau^1, \\ D^5 &= i\mathbb{1}, & D^7 &= i\tau^3, & D^9 &= i\tau^1. \end{aligned} \quad (\text{C7})$$

The generators are normalized as follows

$$\text{Tr} [S^a S^b] = \frac{1}{2} \delta^{ab}, \quad \text{Tr} [X^i X^j] = \frac{1}{2} \delta^{ij}, \quad \text{Tr} [X^i S^a] = 0. \quad (\text{C8})$$

- 
- [1] M. E. Shaposhnikov, “Possible Appearance of the Baryon Asymmetry of the Universe in an Electroweak Theory,” *JETP Lett.* **44**, 465 (1986) [*Pisma Zh. Eksp. Teor. Fiz.* **44**, 364 (1986)].
- [2] M. E. Shaposhnikov, “Baryon Asymmetry of the Universe in Standard Electroweak Theory,” *Nucl. Phys. B* **287**, 757 (1987).
- [3] M. E. Shaposhnikov, “Structure of the High Temperature Gauge Ground State and Electroweak Production of the Baryon Asymmetry,” *Nucl. Phys. B* **299**, 797 (1988).
- [4] G. R. Farrar and M. E. Shaposhnikov, “Baryon Asymmetry Of The Universe In The Minimal Standard Model,” *Phys. Rev. Lett.* **70**, 2833 (1993) [Erratum-*ibid.* **71**, 210 (1993)] [arXiv:hep-ph/9305274].
- [5] G. R. Farrar and M. E. Shaposhnikov, “Baryon Asymmetry Of The Universe In The Standard Electroweak Theory,” *Phys. Rev. D* **50**, 774 (1994) [arXiv:hep-ph/9305275].
- [6] M. B. Gavela, P. Hernandez, J. Orloff and O. Pene, “Standard model CP violation and baryon asymmetry,” *Mod. Phys. Lett. A* **9**, 795 (1994) [arXiv:hep-ph/9312215].
- [7] M. B. Gavela, M. Lozano, J. Orloff and O. Pene, “Standard model CP violation and baryon asymmetry. Part 1: Zero temperature,” *Nucl. Phys. B* **430**, 345 (1994) [arXiv:hep-ph/9406288].
- [8] A. E. Nelson, D. B. Kaplan and A. G. Cohen, “Why there is something rather than nothing: Matter from weak interactions,” *Nucl. Phys. B* **373**, 453 (1992).
- [9] M. Joyce, T. Prokopec and N. Turok, “Efficient Electroweak Baryogenesis From Lepton Transport,” *Phys. Lett. B* **338**, 269 (1994) [arXiv:hep-ph/9401352].
- [10] M. Joyce, T. Prokopec and N. Turok, “Electroweak baryogenesis from a classical force,” *Phys. Rev. Lett.* **75**, 1695 (1995) [Erratum-*ibid.* **75**, 3375 (1995)] [arXiv:hep-ph/9408339].
- [11] M. Joyce, T. Prokopec and N. Turok, “Nonlocal electroweak baryogenesis. Part 1: Thin wall regime,” *Phys. Rev. D* **53**, 2930 (1996) [arXiv:hep-ph/9410281].
- [12] M. Joyce, T. Prokopec and N. Turok, “Nonlocal electroweak baryogenesis. Part 2: The Classical regime,” *Phys. Rev. D* **53**, 2958 (1996) [arXiv:hep-ph/9410282].
- [13] J. M. Cline, K. Kainulainen and A. P. Vischer, “Dynamics of two Higgs doublet CP violation and baryogenesis at the electroweak phase transition,” *Phys. Rev. D* **54**, 2451 (1996) [arXiv:hep-ph/9506284].

- [14] J. M. Cline, “Baryogenesis,” arXiv:hep-ph/0609145.
- [15] M. E. Carrington, “The Effective potential at finite temperature in the Standard Model,” *Phys. Rev. D* **45**, 2933 (1992).
- [16] P. Arnold, “Phase transition temperatures at next-to-leading order,” *Phys. Rev. D* **46**, 2628 (1992) [arXiv:hep-ph/9204228].
- [17] P. Arnold and O. Espinosa, “The Effective potential and first order phase transitions: Beyond leading-order,” *Phys. Rev. D* **47**, 3546 (1993) [Erratum-ibid. *D* **50**, 6662 (1994)] [arXiv:hep-ph/9212235].
- [18] G. W. Anderson and L. J. Hall, “The Electroweak Phase Transition And Baryogenesis,” *Phys. Rev. D* **45**, 2685 (1992).
- [19] M. Dine, R. G. Leigh, P. Y. Huet, A. D. Linde and D. A. Linde, “Towards the theory of the electroweak phase transition,” *Phys. Rev. D* **46**, 550 (1992) [arXiv:hep-ph/9203203].
- [20] K. Kajantie, M. Laine, K. Rummukainen and M. E. Shaposhnikov, “The Electroweak Phase Transition: A Non-Perturbative Analysis,” *Nucl. Phys. B* **466**, 189 (1996) [arXiv:hep-lat/9510020].
- [21] S. Weinberg, “Implications Of Dynamical Symmetry Breaking: An Addendum,” *Phys. Rev. D* **19**, 1277 (1979).
- [22] L. Susskind, “Dynamics Of Spontaneous Symmetry Breaking In The Weinberg-Salam Theory,” *Phys. Rev. D* **20**, 2619 (1979).
- [23] F. Sannino, “Dynamical Stabilization of the Fermi Scale: Phase Diagram of Strongly Coupled Theories for (Minimal) Walking Technicolor and Unparticles,” arXiv:0804.0182 [hep-ph].
- [24] C. T. Hill and E. H. Simmons, “Strong dynamics and electroweak symmetry breaking,” *Phys. Rept.* **381**, 235 (2003) [Erratum-ibid. **390**, 553 (2004)] [arXiv:hep-ph/0203079].
- [25] K. Lane, “Two lectures on technicolor,” arXiv:hep-ph/0202255.
- [26] F. Sannino and K. Tuominen, “Orientifold theory dynamics and symmetry breaking,” *Phys. Rev. D* **71**, 051901 (2005) [arXiv:hep-ph/0405209].
- [27] D. D. Dietrich and F. Sannino, “Conformal window of SU(N) gauge theories with fermions in higher dimensional representations,” *Phys. Rev. D* **75**, 085018 (2007) [arXiv:hep-ph/0611341].
- [28] T. A. Ryttov and F. Sannino, “Conformal Windows of SU(N) Gauge Theories, Higher Dimensional Representations and The Size of The Unparticle World,” *Phys. Rev. D* **76**, 105004 (2007) [arXiv:0707.3166 [hep-th]].

- [29] T. A. Ryttov and F. Sannino, “Supersymmetry Inspired QCD Beta Function,” arXiv:0711.3745 [hep-th]. Physical Review D, in press.
- [30] B. Holdom, “Technicolor,” Phys. Lett. B **150**, 301 (1985).
- [31] E. Eichten and K. D. Lane, “Dynamical Breaking Of Weak Interaction Symmetries,” Phys. Lett. B **90**, 125 (1980).
- [32] B. Holdom, “Raising The Sideways Scale,” Phys. Rev. D **24**, 1441 (1981).
- [33] K. Yamawaki, M. Bando and K. i. Matumoto, “Scale Invariant Technicolor Model And A Technidilaton,” Phys. Rev. Lett. **56**, 1335 (1986).
- [34] T. W. Appelquist, D. Karabali and L. C. R. Wijewardhana, “Chiral Hierarchies and the Flavor Changing Neutral Current Problem in Technicolor,” Phys. Rev. Lett. **57**, 957 (1986).
- [35] K. D. Lane and E. Eichten, “Two Scale Technicolor,” Phys. Lett. B **222**, 274 (1989).
- [36] D. D. Dietrich, F. Sannino and K. Tuominen, “Light composite Higgs from higher representations versus electroweak precision measurements: Predictions for LHC,” Phys. Rev. D **72**, 055001 (2005) [arXiv:hep-ph/0505059].
- [37] R. Foadi, M. T. Frandsen, T. A. Ryttov and F. Sannino, “Minimal Walking Technicolor: Set Up for Collider Physics,” Phys. Rev. D **76**, 055005 (2007) [arXiv:0706.1696 [hep-ph]].
- [38] R. Foadi, M. T. Frandsen and F. Sannino, “Constraining Walking and Custodial Technicolor,” Phys. Rev. D **77**, 097702 (2008) [arXiv:0712.1948 [hep-ph]].
- [39] N. D. Christensen and R. Shrock, “Technifermion representations and precision electroweak constraints,” Phys. Lett. B **632**, 92 (2006) [arXiv:hep-ph/0509109].
- [40] S. Catterall, J. Giedt, F. Sannino and J. Schneible, “Phase diagram of SU(2) with 2 flavors of dynamical adjoint quarks,” arXiv:0807.0792 [hep-lat].
- [41] S. Catterall and F. Sannino, “Minimal walking on the lattice,” Phys. Rev. D **76**, 034504 (2007) [arXiv:0705.1664 [hep-lat]].
- [42] Y. Shamir, B. Svetitsky and T. DeGrand, “Zero of the discrete beta function in SU(3) lattice gauge theory with color sextet fermions,” arXiv:0803.1707 [hep-lat].
- [43] L. Del Debbio, A. Patella and C. Pica, “Higher representations on the lattice: numerical simulations. SU(2) with adjoint fermions,” arXiv:0805.2058 [hep-lat].
- [44] L. Del Debbio, M. T. Frandsen, H. Panagopoulos and F. Sannino, “Higher representations on the lattice: perturbative studies,” JHEP **0806**, 007 (2008) [arXiv:0802.0891 [hep-lat]].
- [45] T. Appelquist, G. T. Fleming and E. T. Neil, “Lattice Study of the Conformal Window in

- QCD-like Theories,” Phys. Rev. Lett. **100**, 171607 (2008) [arXiv:0712.0609 [hep-ph]].
- [46] A. Deuzeman, M. P. Lombardo and E. Pallante, “The physics of eight flavours,” arXiv:0804.2905 [hep-lat].
- [47] S. Nussinov, “Technocosmology: Could A Technibaryon Excess Provide A ‘Natural’ Missing Mass Candidate?,” Phys. Lett. B **165**, 55 (1985).
- [48] S. M. Barr, R. S. Chivukula and E. Farhi, “Electroweak Fermion Number Violation And The Production Of Stable Particles In The Early Universe,” Phys. Lett. B **241**, 387 (1990).
- [49] S. B. Gudnason, C. Kouvaris and F. Sannino, “Dark matter from new technicolor theories,” Phys. Rev. D **74**, 095008 (2006) [arXiv:hep-ph/0608055].
- [50] M. E. Shaposhnikov, “Standard Model Solution Of The Baryogenesis Problem,” Phys. Lett. B **277**, 324 (1992) [Erratum-ibid. B **282**, 483 (1992)].
- [51] V. A. Kuzmin, V. A. Rubakov and M. E. Shaposhnikov, “Electroweak baryogenesis,” *In \*Moscow 1991, Proceedings, Sakharov memorial lectures in physics, vol. 2\* 779-789*
- [52] M. E. Shaposhnikov, “Sphaleron induced baryon number nonconservation,” Nucl. Phys. Proc. Suppl. **26**, 78 (1992).
- [53] J. Bagnasco, M. Dine and S. D. Thomas, “Detecting technibaryon dark matter,” Phys. Lett. B **320**, 99 (1994) [arXiv:hep-ph/9310290].
- [54] C. Kouvaris, “The Dark Side of Strong Coupled Theories,” arXiv:0807.3124 [hep-ph].
- [55] D. S. Akerib *et al.* [CDMS Collaboration], “First results from the cryogenic dark matter search in the Soudan Underground Lab,” Phys. Rev. Lett. **93**, 211301 (2004) [arXiv:astro-ph/0405033].
- [56] D. S. Akerib *et al.* [CDMS Collaboration], “Limits on spin-independent WIMP nucleon interactions from the two-tower run of the Cryogenic Dark Matter Search,” Phys. Rev. Lett. **96**, 011302 (2006) [arXiv:astro-ph/0509259].
- [57] C. Kouvaris, “Dark Majorana Particles from the Minimal Walking Technicolor,” Phys. Rev. D **76**, 015011 (2007) [arXiv:hep-ph/0703266].
- [58] M. Y. Khlopov and C. Kouvaris, “Strong Interactive Massive Particles from a Strong Coupled Theory,” Phys. Rev. D **77**, 065002 (2008) [arXiv:0710.2189 [astro-ph]].
- [59] C. Kouvaris, “WIMP Annihilation and Cooling of Neutron Stars,” Phys. Rev. D **77**, 023006 (2008) [arXiv:0708.2362 [astro-ph]].
- [60] K. Kainulainen, K. Tuominen and J. Virkajarvi, “The WIMP of a minimal technicolor theory,”



- Phys. Rev. D **75**, 085003 (2007) [arXiv:hep-ph/0612247].
- [61] J. M. Cline, “Electroweak phase transition and baryogenesis,” arXiv:hep-ph/0201286.
- [62] Y. Kikukawa, M. Kohda and J. Yasuda, “First-order restoration of  $SU(N_f) \times SU(N_f)$  chiral symmetry with large  $N_f$  and Electroweak phase transition,” Phys. Rev. D **77**, 015014 (2008) [arXiv:0709.2221 [hep-ph]].
- [63] T. Appelquist and F. Sannino, “The physical spectrum of conformal  $SU(N)$  gauge theories,” Phys. Rev. D **59**, 067702 (1999) [arXiv:hep-ph/9806409].
- [64] R. Foadi and F. Sannino, “WW Scattering in Walking Technicolor,” arXiv:0801.0663 [hep-ph]. Physical Review D, in press.
- [65] E. Witten, “An  $SU(2)$  anomaly,” Phys. Lett. B **117**, 324 (1982).
- [66] T. Appelquist, P. S. Rodrigues da Silva and F. Sannino, “Enhanced global symmetries and the chiral phase transition,” Phys. Rev. D **60**, 116007 (1999) [arXiv:hep-ph/9906555].
- [67] D. K. Hong, S. D. H. Hsu and F. Sannino, “Composite Higgs from higher representations,” Phys. Lett. B **597**, 89 (2004) [arXiv:hep-ph/0406200].
- [68] L. Randall, “ETC with a GIM mechanism,” Nucl. Phys. B **403**, 122 (1993) [arXiv:hep-ph/9210231].
- [69] N. Evans and F. Sannino, “Minimal walking technicolour, the top mass and precision electroweak measurements,” arXiv:hep-ph/0512080.
- [70] E. H. Simmons, “Phenomenology Of A Technicolor Model With Heavy Scalar Doublet,” Nucl. Phys. B **312**, 253 (1989).
- [71] M. Dine, A. Kagan and S. Samuel, “Naturalness In Supersymmetry, Or Raising The Supersymmetry Breaking Scale,” Phys. Lett. B **243**, 250 (1990).
- [72] A. Kagan and S. Samuel, “The Family mass hierarchy problem in bosonic technicolor,” Phys. Lett. B **252**, 605 (1990); “Renormalization group aspects of bosonic technicolor,” Phys. Lett. B **270**, 37 (1991).
- [73] C. D. Carone and E. H. Simmons, “Oblique corrections in technicolor with a scalar,” Nucl. Phys. B **397**, 591 (1993) [arXiv:hep-ph/9207273].
- [74] C. D. Carone and H. Georgi, “Technicolor with a massless scalar doublet,” Phys. Rev. D **49**, 1427 (1994) [arXiv:hep-ph/9308205].
- [75] S. B. Gudnason, T. A. Rytov and F. Sannino, “Gauge coupling unification via a novel technicolor model,” Phys. Rev. D **76**, 015005 (2007) [arXiv:hep-ph/0612230].

- [76] J. M. Cline and P. A. Lemieux, “Electroweak phase transition in two Higgs doublet models,” *Phys. Rev. D* **55**, 3873 (1997) [arXiv:hep-ph/9609240]; L. Fromme, S. J. Huber and M. Seniuch, “Baryogenesis in the two-Higgs doublet model,” *JHEP* **0611**, 038 (2006) [arXiv:hep-ph/0605242].
- [77] A. R. Zerwekh, “Associate Higgs and gauge boson production at hadron colliders in a model with vector resonances,” *Eur. Phys. J. C* **46**, 791 (2006) [arXiv:hep-ph/0512261].
- [78] A. Belayev, R. Foadi, M.T. Frandsen, M. Järvinen, A. Pukhov, F. Sannino, to appear.
- [79] A. Mocsy, F. Sannino and K. Tuominen, “Confinement versus chiral symmetry,” *Phys. Rev. Lett.* **92**, 182302 (2004) [arXiv:hep-ph/0308135].
- [80] The reader will find in Appendix F of [23] a complete account of alternative large N limits one can use to gain information on the spectrum of theories with matter in higher dimensional representation
- [81] there may be situations in which the technibaryon is a goldstone boson of an enhanced flavor symmetry
- [82] Another nonminimal way to give masses to the ordinary fermions is to (re)introduce a new Higgs doublet as already done many times in the literature [70, 71, 72, 73, 74, 75]. This possibility and its phenomenological applications will be studied elsewhere.
- [83] The difference between black and white regions is due to the fact that in the black region one still observes a phase transition as function of the temperature while in the white region no phase transition is found for any temperature which is a clear indication of the full breakdown of the high-temperature expansion. Either way these two regions are not accessible within our approximations.